# MIT Open Access Articles

## *Formation of nanoparticles of blue haze enhanced by anthropogenic pollution*

**Massachusetts Institute of Technology**

# Formation of nanoparticles of blue haze enhanced by anthropogenic pollution

Renyi Zhang[a,1], Lin Wang[a], Alexei F. Khalizov[a], Jun Zhao[a], Jun Zheng[a], Robert L. McGraw[b], and Luisa T. Molina[c,d]

[a]Department of Atmospheric Sciences and Department of Chemistry, Texas A&M University, College Station, TX 77843; [b]Atmospheric Sciences Division, Brookhaven National Laboratory, Upton, NY 11973-5000; [c]Molina Center for Energy and the Environment, La Jolla, CA 92093; and [d]Massachusetts Institute of Technology, Cambridge, MA 02139

The molecular processes leading to formation of nanoparticles of blue haze over forested areas are highly complex and not fully understood. We show that the interaction between biogenic organic acids and sulfuric acid enhances nucleation and initial growth of those nanoparticles. With one *cis*-pinonic acid and three to five sulfuric acid molecules in the critical nucleus, the hydrophobic organic acid part enhances the stability and growth on the hydrophilic sulfuric acid counterpart. Dimers or heterodimers of biogenic organic acids alone are unfavorable for new particle formation and growth because of their hydrophobicity. Condensation of low-volatility organic acids is hindered on nano-sized particles, whereas ammonia contributes negligibly to particle growth in the size range of 3–30 nm. The results suggest that initial growth from the critical nucleus to the detectable size of 2–3 nm most likely occurs by condensation of sulfuric acid and water, implying that anthropogenic sulfur emissions (mainly from power plants) strongly influence formation of terrestrial biogenic particles and exert larger direct and indirect climate forcing than previously recognized.

aerosol | biogenic | climate | nucleation | forest

Forests emit an enormous amount of nonmethane hydrocarbons, such as monoterpenes that have a global emission rate on the order of $10^{14}$ g $yr^{-1}$ (1). The $\alpha$- and $\beta$-pinenes are the two most abundant monoterpenes in the troposphere, accounting for $\approx$60% of the total terpene budget. Went (2) first recognized the phenomenon of blue haze over forests, and attributed its formation to biogenic plant emissions. The monoterpenes react with atmospheric oxidants to form a number of products (3, 4), some of which undergo gas-to-particle conversion to form secondary aerosols. Aerosols formed over forested areas contribute importantly to the global aerosol burden, and impact the climate directly by scattering incoming solar radiation, indirectly by altering cloud formation as cloud-condensation nuclei (CCN), or by being involved in multiphase atmospheric chemical processes (5–7).

Biogenic hydrocarbons likely promote secondary aerosol formation in several distinct ways. Photochemical oxidation of biogenic hydrocarbons leads to formation of low-volatility products that likely contribute to particle nucleation. For example, pinonic acids have been suggested as important products from $\alpha$-pinene reaction with ozone (8). Field measurements indicated that pinonic acids represent an important constituent of nano-sized particles over forests (9). Also, oxygenated organic species, which are formed from oxidation of biogenic hydrocarbons (10–12), may engage in heterogeneous reactions to lead to aerosol growth (13–15).

Several mechanisms have been proposed to explain nucleation events in the continental troposphere, including binary $H_2SO_4/H_2O$ and ternary $H_2SO_4/H_2O/NH_3$ nucleation (16), ion-induced nucleation (17, 18), and nucleation enhanced by aromatic organic acids (19). Sulfuric acid has been widely identified as a major atmospheric nucleating species (20, 21). New particle formation is kinetically limited by the population of critical nuclei (22), but little is known about the chemical compositions of the critical nuclei and the identity of other species that also participate in nucleation. Another area of major uncertainty in new particle formation is the mechanism of the initial growth from the critical nucleus to the detectable size of 2–3 nm. Compounds that have been suggested as the likely candidates for nano-sized particle growth include ammonia and organics, in addition to sulfuric acid (22).

## Results and Discussion

We conducted experimental and theoretical studies to investigate nucleation and initial growth of nano-sized biogenic aerosols over forests. Biogenic organic acids including *cis*-pinonic acid (CPA) and their mixtures with sulfuric acid and water were used as a model system to mimic nucleation of biogenic particles (23) in an aerosol chamber. Aerosols ($>$2 nm) were generated when gaseous $H_2SO_4$ was delivered into the nucleation chamber along with a humidified nitrogen carrier gas, and the particle size and distribution were determined by using a nano-differential mobility analyzer (DMA). A pronounced increase in new particle formation over the $H_2O/H_2SO_4$ binary system occurred when CPA was introduced at a concentration on the order of $10^8$–$10^9$ molecule $cm^{-3}$. Fig. 1*A* shows that the measured particle size ranges from 2 to 4 nm, with a variable peak size depending primarily on the $H_2SO_4$ concentration. The nucleation rate increased with CPA and $H_2SO_4$ concentrations (Fig. 1 *B–E*).

In the absence of sulfuric acid, no new particle formation occurred, even when the concentration of CPA reached a value of 20–30 times higher than its saturation concentration of $\approx$1.7 $\times$ $10^{10}$ molecule $cm^{-3}$ at room temperature. Additional experiments were performed to survey new particle formation with the coexistence of two different organic acids, including pinic and norpinic acids that are also coproducts of $\alpha$-pinene ozonolysis (8). A previous environmental chamber study suggested that organic aerosol nucleation might occur through formation of stable organic heterodimers (24). On the basis of analysis of the molecular composition of particle-phase ozonolysis products of $\alpha$-pinene, the formation of difunctional carboxylic acids was shown to govern most of the mass in the particle-phase. A strong intermolecular force between different diacids was suggested to play a key role in the formation of initial nuclei and their subsequent growth. We did not detect new particle formation using a combination of two of the three organic acids with the concentrations of the organic acids as high as 5 $\times$ $10^{11}$ molecule $cm^{-3}$ ($\approx$20 parts per billion) in the nucleation chamber.
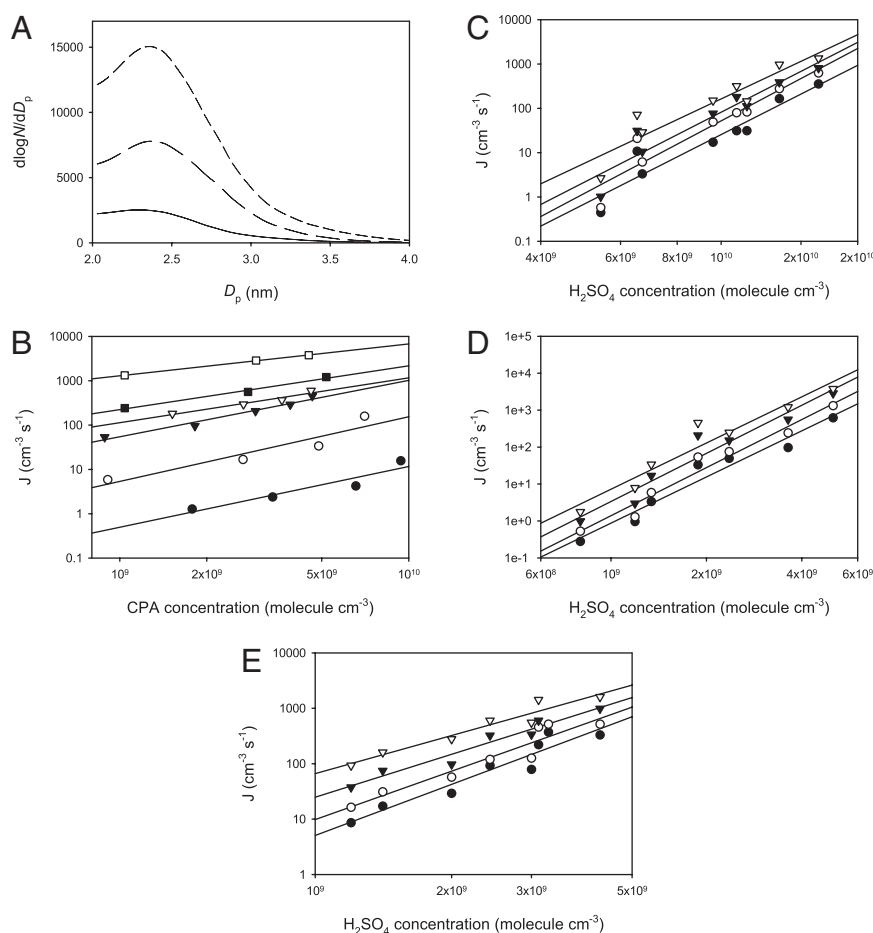
**Fig. 1.** New particle formation in the presence of CPA, $H_2SO_4$, and $H_2O$. (*A*) Size distribution of newly nucleated particles. The concentration of $H_2SO_4$ was $\approx 3 \times 10^9$ molecule $cm^{-3}$, and the relative humidity (RH) was at 20%. The concentration of CPA was $7.2 \times 10^9$ molecule $cm^{-3}$ for top curve (short dashed line), $4.9 \times 10^9$ molecule $cm^{-3}$ for middle curve (long-dashed line), and zero for bottom curve (solid line). (*B*) Nucleation rate (*J*) as a function of CPA concentrations at 13% RH. For the lines from top to bottom, the $H_2SO_4$ concentration varied from $5 \times 10^9$ (open squares), $3.6 \times 10^9$ (solid squares), $2.4 \times 10^9$ (open triangles), $1.9 \times 10^9$ (solid triangles), $1.3 \times 10^9$ (open circles) to $0.8 \times 10^9$ molecule $cm^{-3}$ (solid circles). (*C–E*) Nucleation rate as a function of the $H_2SO_4$ concentration at RH of 6% (*C*), 13% (*D*), and 20% (*E*). For the lines from top to bottom in *C*, the CPA concentration varied from $2.1 \times 10^9$ (open triangles), $1.1 \times 10^9$ (solid triangles), and $5.4 \times 10^8$ molecule $cm^{-3}$ (open circles) to zero (solid circles). For the lines from top to bottom in *D*, the CPA concentration varied from $6.1 \times 10^9$ (open triangles), $4.0 \times 10^9$ (solid triangles), and $1.4 \times 10^9$ molecule $cm^{-3}$ (open circles) to zero (solid circles). For the lines from top to bottom in *E*, the CPA concentration varied from $7.1 \times 10^9$ (open triangles), $4.9 \times 10^9$ (solid triangles), and $1.7 \times 10^9$ molecule $cm^{-3}$ (open circles) to zero (solid circles). All experiments were performed at $284 \pm 2$ K and a total pressure of 760 Torr.

We used the nucleation theorem to estimate the molecular composition in the critical nucleus on the basis of measurements of the vapor phase concentrations and nucleation rates (25). The analyses yielded one CPA and three to five sulfuric acid molecules in the critical nucleus. Quantum chemical calculations have demonstrated the existence of a stable complex between organic acid and $H_2SO_4$ molecules, characterized by strong double-hydrogen bonding (23). The stability of the CPA-$H_2SO_4$ complex is much higher than those of the $H_2O$-$H_2SO_4$, $H_2SO_4$-$NH_3$, and $H_2SO_4$-$H_2SO_4$ complexes; the bonding energy of the CPA-$H_2SO_4$ complex is $\approx 4$–7 kcal $mol^{-1}$ higher than those of the $H_2O$-$H_2SO_4$, $H_2SO_4$-$NH_3$, and $H_2SO_4$-$H_2SO_4$ complexes. Also, the dipole moment of the CPA-$H_2SO_4$ complex (4.6 Debye) is larger than those of the $H_2O$-$H_2SO_4$ and $H_2SO_4$-$H_2SO_4$ complexes, enhancing dipole-dipole interaction with polar molecules such as $H_2SO_4$ and $H_2O$ (26). The large size, bonding energy, and dipole moment of the CPA-$H_2SO_4$ complex likely enhance successive condensations of $H_2SO_4$ and $H_2O$ molecules to form the critical nucleus.

Fig. 2 shows molecular dynamic simulation of a critical nucleus of the CPA-$H_2SO_4$-$H_2O$ system. From the CPA-$H_2SO_4$ complex

to the critical nucleus, the size of the cluster increases from 1.1 to 1.4 nm. It is evident that the sulfuric acid part of the complex is hydrophilic, corresponding exclusively to the growth of the cluster. Conversely, the CPA portion of the complex is hydrophobic that prevents interaction with additional molecules. Except for the carboxylic function group -C(O)OH, the remaining structure of the organic acid is fully saturated. For example, a CPA-CPA dimer also exists that corresponds to a stable complex by forming double-hydrogen bonding between the two carboxylic functional groups from each CPA molecule (23), but such a complex is completely saturated and hydrophobic, inhibiting further cluster growth. The dominant hydrophobic nature of organic acids likely explains the existence of only one CPA molecule in the critical nucleus. This behavior also implies that dimers or heterodimers of organic acids alone are unfavorable for new particle formation because of their hydrophobicity, consistent with our experimental observation of no new particle formation in the coexistence of two supersaturated organic acid vapors.

We performed experiments to analyze the chemical compositions of nano-size particles to gain insight into the nucleation process by using a thermal desorption–ion drift chemical ion-
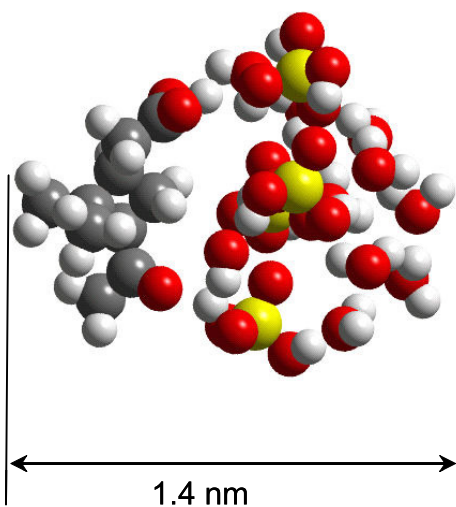
**Fig. 2.** Molecular dynamic simulation of a critical nucleus consisting of one CPA, four sulfuric acid, and 10 water molecules. Carbon, sulfur, oxygen, and hydrogen atoms are represented by black, yellow, red, and gray spheres, respectively. The organic acid portion (*Left*) is connected to the cluster via the carboxylic functional group.

ization mass spectrometer (TD-ID-CIMS) (27–29). The presence of sulfuric acid and CPA is clearly evident in the desorption spectra, showing the characteristics of $H_2SO_4$, $H_2SO_4$-$H_2SO_4$ dimer, CPA, and CPA-$H_2SO_4$ dimer (Fig. 3). However, sulfuric acid ($H_2SO_4$ and $H_2SO_4$-$H_2SO_4$ dimer) is far more abundant than CPA (CPA and CPA-$H_2SO_4$ dimer) from the desorbed mass, with a mass ratio of ≈1,000 to 1 between $H_2SO_4$ and CPA. The dominance of $H_2SO_4$ in the nanoparticles is explained by its large sticking coefficient and high affinity for water (30, 31). In general, condensation of low-volatility species on nano-sized particles is greatly suppressed because of enormously elevated equilibrium vapor pressures from the curvature (Kelvin) effect (31). However, $H_2SO_4$ molecules condensed on newly nucleated particles are efficiently stabilized by simultaneous condensation of $H_2O$ molecules, which prevents evaporation of $H_2SO_4$ and leads to an irreversible growth process. In contrast, condensation of CPA on nano-sized particles is limited because of its hydrophobicity and lack of stabilization. Thus, the initial growth from the critical nucleus to the detectable 2–3 nm particles occurs exclusively by condensations of $H_2SO_4$ and $H_2O$. While enhancing the formation of the critical nucleus by forming a stable complex with sulfuric acid, organic acids contribute negligibly to growth of newly nucleated nanoparticles.

Growth of particles in the size range of 3–30 nm was further studied in the presence of ammonia using a nano-tandem (T)DMA. The sizes of monodisperse particles before and after exposure to ammonia were measured, and the ratio of the two particle sizes yielded the particle growth factor (Fig. 4). Growth of particles of 3–30 nm by exposure to ammonia is negligible over a range of relative humidity conditions. Although it is plausible that the heterogeneous reaction between ammonia and sulfuric acid occurs to produce ammonium sulfate [$(NH_4)_2SO_4$] on larger particles, ammonium sulfate has a larger density than that of sulfuric acid (30), and its formation does not necessarily contribute to a net increase in the particle size.

In our previous work we have suggested that several aromatic acids, produced from photochemical oxidation of aromatic hydrocarbons, enhance aerosol nucleation (19). The present study extends that work and provides insights into the molecular
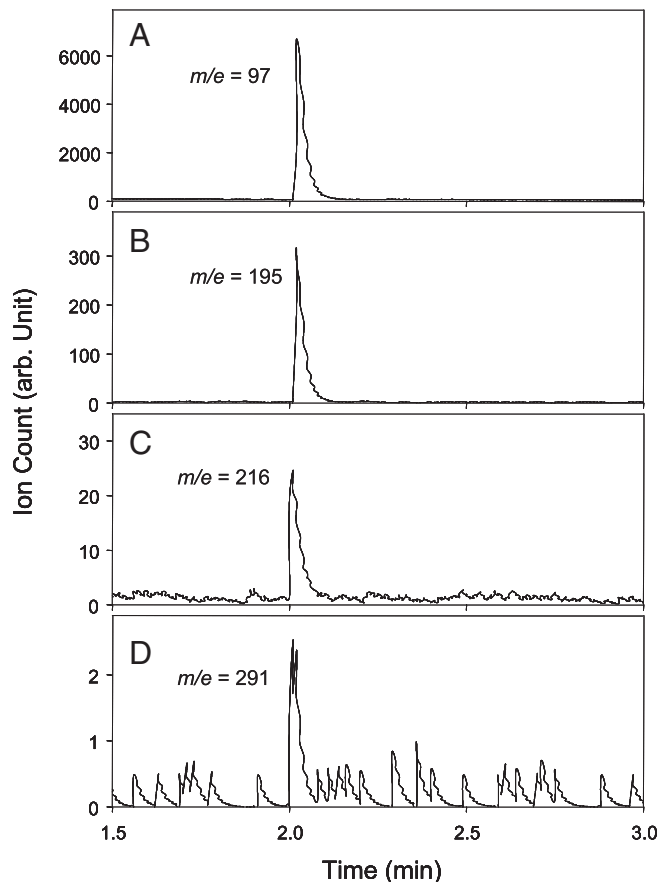


**Fig. 3.** TD-ID-CIMS composition analysis of nano-sized particles formed from the ternary nucleation of the $H_2SO_4$-CPA-$H_2O$ system. Ion signals for $HSO_4^-$, $HSO_4^-$·$H_2SO_4$, CPA·$O_2^-$, and $HSO_4^-$·CPA, representing $H_2SO_4$, $H_2SO_4$-$H_2SO_4$ dimer, CPA, and CPA-$H_2SO_4$ dimer, respectively. The reagent ions were $CO_3^-$ (60 amu) and $CO_4^-$ (76 amu). The collected particle mass was heated at ≈2 min. To ensure a sufficient mass was collected, the particle size ranged from 3 to 13 nm, with a peak diameter of ≈7 nm and a peak concentration (d$N$/d$Dp$) of $10^7$. The ratio between CPA and $H_2SO_4$ was estimated to be ≈1 to1,000 in the collected particle mass. In our experiments, it took ≈4 h to collect a ≈150 ng particle mass, assuming a 10% overall charging efficiency and a particle density of 1.5 g cm$^{-3}$.

processes leading to nucleation and growth of nano-sized aerosols over forests. Oxidation of biogenic monoterpenes yields organic acids such as CPA that contribute to new particle formation. The hydrophobic organic acid part in the CPA-sulfuric acid complex results in large stability and enhances growth on the hydrophilic sulfuric acid counterpart to form the critical nucleus. In contrast to the previous studies (24), our results demonstrate that dimers or heterodimers of organic acids alone cannot lead to new particle formation, because since growth from such complexes is prohibited because of their hydrophobicity and the Kelvin effect. By differentiating the processes between nucleation and growth of newly nucleated nano-sized particles, we show that the initial growth from the critical nucleus to the detectable size of 2–3 nm takes place mainly from condensation of $H_2SO_4$, along with simultaneous condensation of $H_2O$, but unlikely from condensation of low volatility organic acids or interaction with ammonia. The present analysis of the chemical compositions of newly nucleated aerosols and molecular dynamic simulations provide insights into the molecular information of the critical nucleus, indicating that the critical nucleus likely consists of one CPA and three to five sulfuric acid molecules, along with $H_2O$ molecules. Ambient
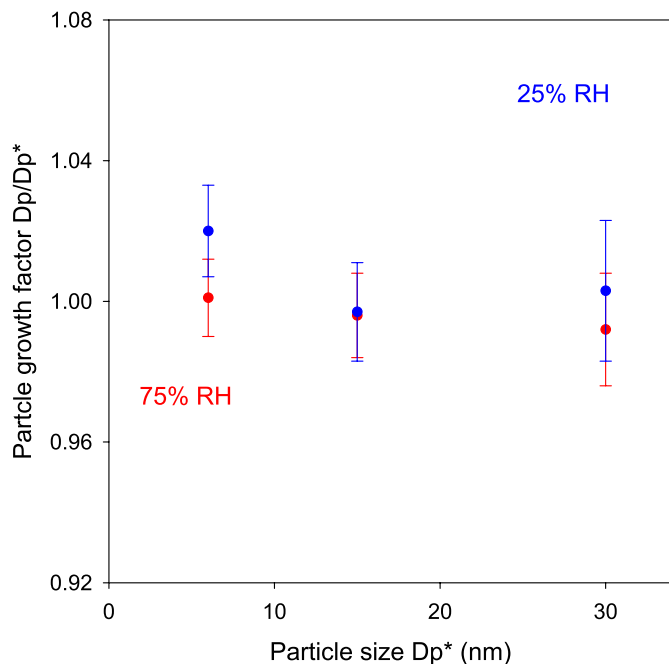
**Fig. 4.** Growth factor ($D_p/D_p*$) of particles on exposure to ammonia under different RH conditions, where $D_p*$ denotes the initial particle size selected by the first nano-DMA, and $D_p$ represents the particle size measured by the second nano-DMA after exposure. The exposure time was ≈30 s. The gaseous concentration of ammonia was $3 \times 10^{14}$ molecule cm$^{-3}$. The experiments were performed at 2 RH conditions, i.e., 25% (blue) and 75% (red), 298 ± 2 K, and 760 Torr. The vertical bars represented the random error of the measurements (2 $\sigma$), and the values were averaged over at least three measurements.

measurements indirectly inferred a linear or square dependence of the nucleation rate on the $H_2SO_4$ concentration (20), but a cluster consisting of one or two sulfuric acid and water molecules alone unlikely corresponds to a critical nucleus without the presence of other species. Also, the dominant abundance of $H_2SO_4$ in the nano-sized particles implies that the subsequently grown aerosols can be hygroscopic.

Sulfur dioxide has an atmospheric gas-phase lifetime on the order of several days and is transported throughout the continental troposphere; emissions of sulfur dioxide have been considerably increased over the past century because of coal burning from power plants (3, 32). Field measurements in remote forest sites showed that new particle formation was closely correlated with elevated production of gaseous sulfuric acid (33), consistent with recent laboratory experiments showing the role of sulfuric acid in aerosol nucleation (34–36). Our results show that the interaction between sulfuric acid and biogenic organic acids enhances both nucleation and initial growth of nano-sized particles, indicating that anthropogenic pollution strongly impacts aerosol formation over pristine

forested areas. Also, organic aerosols are generally considered to be less hygroscopic, whereas the aerosol hygroscopicity determines their effects on interference with solar radiation transfer and cloud formation (5). The present laboratory experiments reveal the dominant role of sulfuric acid in the initial growth of nano-sized particles, which can influence the hygroscopic characteristics of biogenic aerosols. The strong interaction between terrestrial biogenic and anthropogenic sulfur emissions implies that terrestrial biogenic aerosols over forested areas likely exert larger direct and indirect climate forcing than previously recognized.

## Methods

The laboratory setup for the nucleation experiments consisted of a nucleation chamber where gaseous aerosol precursors were introduced, an ID-CIMS for monitoring the concentrations of gaseous species, a nano-DMA for measurements of the size and distribution of aerosols, and TD-ID-CIMS for analysis of the chemical compositions of aerosols. A detailed description of the nucleation system is provided elsewhere (19).

The chemical composition of nano-sized particles was analyzed by TD-ID-CIMS. Newly nucleated particles generated in the nucleation chamber were charged and electrostatically deposited on a charged platinum wire. The collected particle mass was subsequently heated/evaporated and analyzed by using TD-ID-CIMS.

The growth of particles was measured by using nano-TDMA. Aerosols were produced from the binary $H_2SO_4/H_2O$ nucleation and size-selected using a nano-DMA ($D_p*$). Subsequently, the monodisperse particles were introduced into a growth chamber, where they were exposed to ammonia vapor on the time scale of ≈30 s. A second nano-DMA was then used to sample the aerosol flow at the end of the growth chamber ($D_p$), and the ratio of the particle sizes measured by the two nano-DMAs ($D_p/D_p*$) yielded the particle growth factor.

We performed molecular dynamic simulations using the Cerius$^2$ Open Force Field module (OFF) with the CFF1.02 force field (Accelrys). The molecular clusters were constructed by using the Cerius$^2$ amorphous builder and a unit cubic cell with 100 nm in dimension using the crystal builder. The cluster with fixed composition was located at the center of the cube with periodic boundary for energy minimization to ensure the stability and minimum potential energy of the model cluster. The minimization was performed using Newton–Raphson algorithms, available in the OFF simulation engine. The minimization process was found to be efficient and was typically converged in a single minimization run within a reasonable computational time (within 30 min). It should be pointed out that, because CFF force field fully accounts for hydrogen bonds in the function expression, explicit specification was not required for the clusters with ample hydrogen bonds in this study. The dynamic simulation was performed using the Verlet leapfrog integrator under fixed composition, isobaric and isothermic [number concentration, pressure and temperature, (NPT)] thermodynamic ensemble with periodic boundary condition. The external pressure of the system was set to zero. The size and the shape of the unit cell were allowed to vary to accommodate the adjustment of the pressure (kept at 1 atm), and the temperature was controlled by the T-Damping method. An integration time step of 1 fs was used to ensure the stability and accuracy in the integration process, and the number of $3 \times 10^7$ steps was carried out so that a total simulation time of ≈30 ns was obtained, long enough to capture sufficient representative conformations.

1. Guenther A, et al. (1995) A global-model of natural volatile organic-compound emissions. *J Geophys Res* 100:8873–8892.
2. Went FW (1960) Blue hazes in the atmosphere. *Nature* 187:641–643.
3. Finlayson-Pitts BJ, Pitts JN, Jr (2000) *Chemistry of the Upper and Lower Atmosphere: Theory, Experiments, and Applications* (Academic, San Diego, CA).
4. Zhao J, Zhang R (2008) Theoretical investigation of atmospheric oxidation of biogenic hydrocarbons: A critical review. *Adv Quantum Chem* 55:177–213.
5. Novakov T, Penner JE (1993) Large contribution of organic aerosols to cloud-condensation-nuclei concentrations. *Nature* 365:823–826.
6. Andreae MO, Crutzen PJ (1997) Biogeochemical sources and role in atmospheric chemistry. *Science* 276:1052–1058.
7. Zhang R, Tie X, Bond DW (2003) Impacts of anthropogenic and natural NOx sources over the U.S. on tropospheric chemistry. *Proc Natl Acad Sci USA* 100:1505–1509.
8. Zhang D, Zhang R (2005) Ozonolysis mechanisms of α- and β-pienes: Kinetics and mechanism. *J Chem Phys* 122:114308 (1–12).
9. O'Dowd CD, Aalto P, Hameri K, Kulmala M, Hoffmann T (2002) Aerosol formation - Atmospheric particles from organic vapours. *Nature* 416:497–498.
10. Fan J, Zhang R (2004) Atmospheric oxidation mechanism of isoprene. *Environ Chem* 1:140–149.
11. Suh I, Lei W, Zhang R (2001) Experimental and theoretical studies of isoprene reaction with NO3. *J Phys Chem* 105:6471–6478.
12. Lei W, et al. (2000) Theoretical study of isomeric branching in the isoprene-OH reaction: Implications to final product yields in isoprene oxidation. *Chem Phys Lett* 326:109–114.
13. Zhao J, Levitt NP, Zhang R (2005) Heterogeneous chemistry of octanal and 2, 4-hexadienal with sulfuric acid. *Geophys Res Lett* 32:L09802, doi:10.1029/2004GL022200.
14. Zhao J, Levitt NP, Zhang R, Chen J (2006) Heterogeneous reactions of methylglyoxal in acidic media: Implications for secondary organic aerosol formation. *Environ Sci Technol* 40:7682–7687.

ENVIRONMENTAL SCIENCES

15. Levitt NP, Zhao J, Zhang R (2006) Heterogeneous chemistry of butanol and decanol with sulfuric acid: Implications for secondary organic aerosol formation. *J Phys Chem A* 110:13215–13220.
16. Ball SM, Hanson DR, Eisele FL, McMurry PH (1999) Laboratory studies of particle nucleation: Initial results for $H_2SO_4$, $H_2O$, and $NH_3$ vapors. *J Geophys Res* 104:23709–23718.
17. Yu FQ, Turco RP (2001) From molecular clusters to nanoparticles: Role of ambient ionization in tropospheric aerosol formation. *J Geophys Res* 106:4797–4814.
18. Lee SH, et al. (2003) Particle formation by ion nucleation in the upper troposphere and lower stratosphere. *Science* 301:1886–1889.
19. Zhang R, et al. (2004) Atmospheric new particle formation enhanced by organic acids. *Science* 304:1487–1490.
20. McMurry PH, et al. (2005) A criterion for new particle formation in the sulfur-rich Atlanta atmosphere. *J Geophys Res* 110:D22S02, doi:10.1029/2005JD005901.
21. Zhang Q, et al. (2004) Insights into the chemistry of new particle formation and growth events in Pittsburgh based on aerosol mass spectrometry. *Environ Sci Technol* 38:4797–4809.
22. Kulmala M (2003) How particles nucleate and grow. *Science* 302:1000–1001.
23. Zhao J, Khalizov AF, Zhang R, McGraw R (2009) Hydrogen bonding interaction of molecular complexes and clusters of aerosol nucleation precursors. *J Phys Chem* 113:680–689.
24. Hoffmann T, Bandur R, Marggraf U, Linscheid M (1998) Molecular composition of organic aerosols formed in the alpha-pinene/$O_3$ reaction: Implications for new particle formation processes. *J Geophys Res* 103:25569–25578.
25. McGraw R, Zhang R (2008) Multivariate analysis of homogeneous nucleation rate measurements: I. Nucleation in the p-toluic acid/sulfuric acid/water system. *J Chem Phys* 128:064508, doi:10.1063/1.2830030.
26. Maitland GC, Rigby M, Smith EB, Wakeham WA (1981) *Intermolecular Forces: Their Origin and Determination* (Oxford Univ Press, New York).
27. Smith JN, Moore KF, McMurry PH, Eisele FL (2004) Atmospheric measurements of sub-20 nm diameter particle chemical composition by thermal desorption chemical ionization mass spectrometry. *Aerosol Sci Technol* 38:100–110.
28. Fortner EC, Zhao J, Zhang R (2004) Development of ion drift-chemical ionization mass spectrometry. *Anal Chem* 76:5436–5440.
29. Zhao J, Zhang R (2004) Proton transfer reaction rate constants between hydronium ion ($H_3O^+$) and volatile organic compounds (VOCs). *Atmos Environ* 38:2177–2185.
30. Zhang R, Wooldridge PJ, Abbatt JPD, Molina MJ (1993) Physical chemistry of the $H_2SO_4/H_2O$ binary system at low temperatures: Implications for the stratosphere. *J Phys Chem* 97:7351–7358.
31. Zhang R, et al. (2008) Variability in morphology, hygroscopic and optical properties of soot aerosols during internal mixing in the atmosphere. *Proc Natl Acad Sci USA* 105:10291–10296.
32. Eisele FL, McMurry PH (1997) Recent progress in understanding particle nucleation and growth. *Philos Trans R Soc London B* 352:191–200.
33. Weber RJ, et al. (1997) Measurements of new particle formation and ultrafine particle growth rates at a clean continental site. *J Geophys Res* 103:4375–4385.
34. Benson DR, Erupe ME, Lee SH (2009) Laboratory-measured H2SO4-H2O-NH3 ternary homogeneous nucleation rates: Initial observation. *Geophys Res Lett* 36:L15818, doi:15810.11029/12009gl038728.
35. Benson DR, Young LH, Kameel FR, Lee SH (2008) Laboratory-measured nucleation rates of sulfuric acid and water binary homogeneous nucleation from the SO2+OH reaction. *Geophys Res Lett* 35:L11801, doi:11810.11029/12008gl033387.
36. Young LH, et al. (2008) Laboratory studies of H2SO4/H2O binary homogeneous nucleation from the SO2+OH reaction: Evaluation of the experimental setup and preliminary results. *Atmos Chem Phys* 8:4997–5016.